EVALUATION OF THE ADREA-HF CFD CODE AGAINST A HYDROGEN DEFLAGRATION IN A TUNNEL

Tolias, I.C.[1,2], Venetsanos, A.G.[1] and Markatos, N.[2]
[1] Environmental Research Laboratory, National Center for Scientific Research Demokritos, Agia Paraskevi, 15310, Greece, tolias@ipta.demokritos.gr, venets@ipta.demokritos.gr
[2] National Technical University of Athens, School of Chemical Engineering, Heroon Polytechniou 9, Zografou, 15780, Greece, n.markatos@ntua.gr

ABSTRACT

In the present work, the capabilities of the computational fluid dynamics (CFD) code ADREA-HF to predict deflagration in homogenous, near stoichiometric hydrogen-air mixture in a model of a tunnel were tested. The tunnel is 78.5 m long. Hydrogen-air mixture is located in a 10 m long region in the middle of the tunnel. Two cases are studied: one with a complete empty tunnel and one with the presence of four vehicles near the center of the tunnel. The combustion model is based on the turbulent flame speed concept. The turbulent flame speed is a modification of Yakhot's equation, in order to account for additional physical mechanisms. A sensitivity analysis for the ψ parameter of the combustion model and for the mesh resolution was made for the empty tunnel case.The agreement between experimental and computational results concerning the value of the maximum pressure, and the time it appears, is satisfactory in both cases. The sensitivity analysis for the parameter of the combustion model showed that even small changes in it can have impact on the simulating results, whereas the sensitivity analysis of the mesh resolution did not reveal any significant differences.

NOMENCLATURE

t	Time (sec)	D_f	Fractal dimension
x	Distance (m)	m_0	Temperature index in dependence of burning velocity on pressure
u	Velocity (m/s)	n_0	Pressure index in dependence of burning velocity on pressure
p	Pressure (Pa)	k_{sgs}	Subgrid turbulent kinetic energy (Joule/kg)
g	Gravity (m/s^2)	L_{sgs}	Subgrid length scale (m)
Pr	Prandtl number	*Greek letters*	
D	Diffusivity (m^2/s)	ρ	Mixture density (kg/m^3)
Sc	Schmidt number	μ	Viscosity (kg/m/s)
H	Static enthalpy (Joule)	ν	Stoichiometric coefficient
q	Mass fraction	γ	Adiabatic index
$\overline{R}$	Mean reaction rate (kg/m^3/sec)	Ξ	Wrinkling factors
N_{subs}	Number of species	ψ	Model constant
S_{ij}	Rate of strain tensor (1/sec)	ε	Overall thermokinetic index
V	Volume of computational cell (m^3)	*Subscripts superscripts and bars*	
MW	Molecular weight (gr/mole)	0	Initial conditions
S_t	Turbulent burning velocity (m/s)	u	Unburned mixture
q_f	Fuel mass fraction	t	Turbulent
u'_{sgs}	SGS velocity component (m/s)	max	Maximum
E	Expansion coefficient	$\bar{}$	Filtered quantity

S_u	Laminar flame speed (m/s)	~	Mass-weighted filtered quantity
R_0	Critical radius (m)	pmax	Maximum overpressure
R	Distance (m)	0.1pmax	10% of maximum overpressure

1.0 INTRODUCTION

Hydrogen is a very promising alternative fuel which is expected to play a significant role in the near future. Hydrogen has been used since long time ago in the process industry. Nowadays, hydrogen is considered as an excellent alternative fuel due to its potential to lead to significant reductions in greenhouse gas emissions and significant improvements in energy efficiency. Hydrogen is particularly attractive for vehicle applications. In some countries, hydrogen has already started to be tested in public transportation, e.g. in buses. Limited production of hydrogen fuelled cars has already appeared and a future extensive production of such cars for the general public is expected.

On the other hand, significant safety issues are associated with hydrogen. In the case of an accidental release, hydrogen mixes with air and can form a flammable mixture over a wide range of concentrations, from 4% (lower flammability limit) to 75% (upper flammability limit) per mixture volume. A possible ignition may give rise to slow or fast deflagrations, or even detonations under certain conditions depending on the concentration, the size of the mixture and the geometry involved. Two characteristic catastrophic accidents involving hydrogen explosion is the one that happened in Stockholm in 1983 [1] and the one that happened in Norway in 1985 [2]. The first one was caused by hydrogen release from high pressure interconnected vessels, because of broken connections among them. The second one took place at an ammonia plant when a gasket in a water pump was blown off having as a result the dispersion of 10 to 20 kg of hydrogen. The explosion of hydrogen was violent, destroying the building and killing two men.

In the past years, the increase of computational power has rendered Computational Fluid Dynamics (CFD) as a very attractive methodology for risk assessment of hydrogen applications. With its high accuracy capabilities, CFD can evaluate regulations and standards and provide a new insight. The ADREA-HF code [3], is a well known CFD program which has been extensively validated against hydrogen dispersion applications [4]. Recently, the capabilities of ADREA-HF have been extended to the modelling of turbulent combustion and specifically in the simulation of hydrogen deflagrations. The aim of this work is the evaluation of the ADREA-HF combustion model against a hydrogen deflagration experiment in a tunnel. Overpressure time series measured in the experiment are compared against the computational results. The accurate prediction of the overpressure generated by the explosion is a crucial point in assessing hydrogen safety. However, it is a difficult task as it depends on many factors such as mixture composition, turbulence-chemistry interactions, geometry of the problem and several other physical mechanisms [5].

2.0 EXPERIMENT OVERVIEW

An experiment of hydrogen deflagration in a model of a tunnel was performed by Groethe, Sato et al. [6,7]. Its length is 78.5 m and its cross-section is a part of a 2.4 m diameter circle (Fig. 1). This tunnel is about 1/5 scale of a typical road-tunnel. Various scenarios in the mixture composition and vehicle distribution were performed. In the present work, we examine the case of homogeneous hydrogen-air mixture of 30% hydrogen volumetric concentration, with and without the presence of vehicles in the tunnel. The hydrogen-air mixture is located in a 10 m long region between two sheets of high-density polyethylene in the middle of the tunnel, filling a volume equal to 37 m^3. The ignition location is in the middle of the tunnel. In the non-empty tunnel case, four vehicles are positioned inside the hydrogen-air mixture along the floor centerline as shown in Fig. 1. The distance between vehicles is 1.52 m. The vehicle models dimensions are: 0.94 m in length, 0.362 m in width and 0.343 m in height.

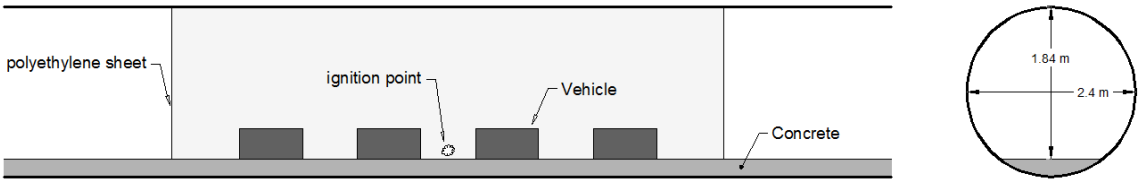

Figure 1. Cross sections of the tunnel model

3.0 MATHEMATICAL METHOLOGY

3.1 Governing equations

The combustion model used, solves the space-averaged Navier-Stokes equations along with the energy equation (conservation equation of static enthalpy) and the conservation equations of each of the mass fraction of the species that take part in the combustion process. The multi-component mixture is assumed to be in thermodynamic equilibrium. The equation of state for ideal gases relates pressure and enthalpy with density and temperature. The set of main equations is:

$$\frac{\partial \bar{\rho}}{\partial t}+\frac{\partial \bar{\rho}\tilde{u}_i}{\partial x_i}=0 \tag{1}$$

$$\frac{\partial \bar{\rho}\tilde{u}_i}{\partial t}+\frac{\partial \bar{\rho}\tilde{u}_j\tilde{u}_i}{\partial x_j}=-\frac{\partial \bar{p}}{\partial x_i}+\frac{\partial}{\partial x_j}\left(\left(\mu+\mu_t\right)\left(\frac{\partial \tilde{u}_i}{\partial x_j}+\frac{\partial \tilde{u}_j}{\partial x_i}\right)\right)+\bar{\rho}g_i,\quad i=1\ldots3 \tag{2}$$

$$\frac{\partial \bar{\rho}\tilde{H}}{\partial t}+\frac{\partial \bar{\rho}\tilde{u}_j\tilde{H}}{\partial x_j}=\frac{\partial}{\partial x_j}\left(\frac{\mu_t}{\mathrm{Pr}_t}\frac{\partial \tilde{H}}{\partial x_j}\right)+\frac{D\bar{p}}{Dt} \tag{3}$$

$$\frac{\partial \bar{\rho}\tilde{q}_k}{\partial t}+\frac{\partial \bar{\rho}\tilde{u}_j\tilde{q}_k}{\partial x_j}=\frac{\partial}{\partial x_j}\left(\frac{\mu_t}{Sc_t}\frac{\partial \tilde{q}_k}{\partial x_j}\right)+\bar{R}_k,\quad k=1,\ldots,N_{subs} \tag{4}$$

The subscripts i,j,k denote the component i, the Cartesian j coordinate and the specie k respectively.

Turbulence is modelled using the RNG-LES model. Derived from the renormalization group theory [8], RNG-LES model has the advantages that it lacks adjustable constants and that it takes into account whether the flow is turbulent or laminar. Its formulation is:

$$\mu_t=\mu\left[1+H\left(\frac{\mu_s^2\mu_t}{\mu^3}-100\right)\right]^{1/3} \tag{5}$$

$$H\left(x\right)=\begin{cases}x, & x>0\\ 0, & x\le 0\end{cases} \tag{6}$$

$$\mu_s=\bar{\rho}\left(0.157\cdot V^{1/3}\right)^2\sqrt{2\tilde{S}_{ij}\tilde{S}_{ij}} \tag{7}$$

$$\tilde{S}_{ij} = \frac{1}{2}\left(\frac{\partial \tilde{u}_i}{\partial x_j} + \frac{\partial \tilde{u}_j}{\partial x_i} \right) \tag{8}$$

The turbulence Prandtl number is calculated from the equation:

$$\frac{\mu}{\mu_t} = \left| \frac{1/\mathrm{Pr}_t - 1.3929}{1/\mathrm{Pr} - 1.3929} \right|^{0.6321} \left| \frac{1/\mathrm{Pr}_t + 2.3929}{1/\mathrm{Pr} + 2.3929} \right|^{0.3679} \tag{9}$$

where the molecular Prandtl number Pr is set equal to 0.72.

3.2 Combustion model

The main issue in premixed combustion modelling is the estimation of the reaction rate which appears in the equation (4) of species as source term. The combustion process occurs typically in a very thin area (flame front) which propagates in space over time. For real case scenarios, this area is very small compared to the length scale of the problem. Consequently, direct numerical simulation with detailed chemistry is not possible at the present. As a result, models for the estimation of the reaction rate need to be developed. The reaction rates of species in equation (4) are not independent from each other but they are correlated through the reaction stoichiometry. For example, all reaction rates can be expressed as a function of the fuel reaction rate as:

$$\bar{R}_i = \frac{\nu_i \cdot MW_i}{\nu_f \cdot MW_f} \cdot \bar{R}_f \tag{10}$$

where subscript i stands for specie i (f for fuel).

The implemented in ADREA_HF code combustion model, originally proposed in [9-11], is based on turbulent flame speed concept [12]. The fuel reaction rate is modelled as follows:

$$\bar{R}_f = \rho_u S_t \left| \nabla q_f \right| \tag{11}$$

The main concern in this type of models is the calculation of the turbulent flame speed. Many equations have been proposed in the literature [13]. A common practice is to correlate the turbulent flame speed to the unresolved component of velocity, u'_{sgs}, to the laminar flame speed, S_u, and to turbulent and chemical length or time scales. Some typical turbulent flame speed equations are introduced by Zimont [12], Schmidt [14], Herweg [15] and Kawanabe [16]. In the utilized model, the calculation of the turbulent flame speed is based on Yakhot's equation for premixed turbulent combustion [17]:

$$S_t = \Xi_k \cdot \Xi_{lp} \cdot \Xi_f \cdot S_u \cdot \exp\left(\frac{u'_{sgs}}{S_t} \right)^2 \tag{12}$$

Yakhot's equation has been derived based on the renormalization group theory [8] and at its original form does not include the Ξ factors. It takes into account the turbulence of the unburned mixture in the incoming flow and the laminar burning velocity. However, it does not account for various flame instabilities which can lead to an increase of the turbulence burning velocity. One mechanism which leads to an acceleration of the flame front, is the turbulence that is generated by the flame front itself. As described in [18] the source of this turbulence is the thermal expansion of the combustion products. The upper limit for a flame wrinkling factor due to the turbulence generated by the flame front itself can be estimated by $\Xi_k^{\max} = (E-1)/\sqrt{3}$ where E is the expansion coefficient. The wrinkling factor,

Ξ_k, gradually increases from the value of one at the ignition point to the maximum value of $\Xi_k^{\max}$ at the critical radius where the turbulence is fully developed. This critical radius is approximately equal to $R_0 = 1.0 - 1.2m$ for near stoichiometric hydrogen-air mixtures [19]. A suggested formula for the wrinkling factor Ξ_k which takes under consideration these parameters is [9]:

$$\Xi_k = 1 + \left(\psi \cdot \Xi_k^{\max} - 1\right) \cdot \left[1 - \exp\left(-R/R_0\right)\right] \tag{13}$$

where R is the distance from the ignition point and ψ is a model constant which represents the level at which the maximum value $\Xi_k^{\max}$ is reached ($0 \le \psi \le 1$). This constant is suggested to be equal to 0.5 for near-stoichiometric mixtures and equal to 1 for lean hydrogen-air mixtures [20]. In the present study we set $R_0 = 1.2$, $E = 7.2$ and we examine two value of ψ , 0.45 and 0.50.

Another mechanism which leads to acceleration of the flame front is the preferential diffusion which appears in mixtures with Lewis number less that one. The development of this thermal-diffusive instability causes an increment of the laminar burning velocity. Based on the work of Zimont and Lipatnikov [21], a correction factor Ξ_{lp} for the laminar burning velocity can be calculated for a given mixture composition. In our case (30% hydrogen concentration) this factor is approximately equal to 1.25. In order to take into account the transition growth of the instability, Ξ_{lp} value was increased linearly from 1 at the ignition point to 1.25 at the distance of $R_0/2$. Elsewhere, the Ξ_{lp} value remained constant and equal to 1.25.

The Ξ_f coefficient is given by the following equation:

$$\Xi_f = \begin{cases} \left(\dfrac{R}{R_0}\dfrac{\varepsilon_{R_0}}{\varepsilon_R}\right)^{D_f - 2} & , \; R \ge R_0 \\ 1 & , \; R < R_0 \end{cases} \tag{14}$$

where ε_{R_0} and ε_R are the inner cut-off scales at R_0 and R respectively. This coefficient accounts for the increase of the flame front surface due to its fractal structure. Details and the expressions of ε_{R_0}, ε_R can be found in [22].

For the calculation of the laminar burning velocity S_u, the dependence on the pressure and temperature is considered by the assumption of adiabatic compression [23]:

$$S_u = S_{u0}\left(\frac{T}{T_{u0}}\right)^{m_0}\left(\frac{P}{P_0}\right)^{n_0} = S_{u0}\left(\frac{P}{P_0}\right)^{\varepsilon} \tag{15}$$

where S_{u0} is the laminar burning velocity at initial composition temperature T_{u0} and pressure P_0 and $\varepsilon = m_0 + n_0 - m_0/\gamma$ is the overall thermokinetic index. The values of ε and S_{u0} are taken as functions of the fuel concentration. The dependence of m_0 , n_0 and S_{u0} on the fuel concentration can be found in [23]. The values of ε used in the present work are taken from [24]. The density of the unburned mixture (ahead of the flame front) ρ_u is calculated by using the assumption of adiabatic compression:

$$\rho_u = \rho_{u0}\left(\frac{p}{p_0}\right)^{1/\gamma} \tag{16}$$

Finally, the sub-grid scale unresolved velocity u'_{sgs} is estimated from the equation:

$$u'_{sgs} = \sqrt{\frac{2}{3}} \cdot \frac{\mu_t}{0.157 \cdot \bar{\rho} \cdot V^{1/3}} \tag{17}$$

This equation can be derived by the subgrid turbulent kinetic energy from the equation $u'_{sgs} = \sqrt{2/3 \cdot k_{sgs}}$ using the assumption of isotropic turbulence. By dimensional analysis, turbulent kinetic energy is equal to $\frac{\mu_t^2}{\rho^2 L_{sgs}^2}$ where $L_{sgs} = 0.157 \cdot V^{1/3}$ is the subgrid length scale.

3.3 Numerical details

ADREA-HF uses the finite volume method on a staggered Cartesian grid. The geometry is reproduced with the use of porosities, which makes possible the correct representation of any solid surface on a structured mesh [25,26]. The pressure and velocity equations are decoupled using a modification of the SIMPLER algorithm [27,28]. For the discretization of the convective terms in the momentum equations a second order accurate bounded central scheme [29] was used (which is a common practise in LES simulations), while in the conservation equations of species and energy a second order accurate bounded linear upwind scheme [29]. This different discretization strategy for the species and the energy equations seems to give better results than the use of the central differences scheme in all equations [30]. The implementation was carried out using a deferred-correction approach via source terms [31,32]. For the time advancement, a second order accurate Crank-Nicolson numerical scheme was chosen. The time step is automatically adapted according to prescribed error bands and desired Courant–Friedrichs–Lewy (CFL) number which was set equal to 0.6. The equation of the turbulent flame speed (12) is solved numerically by Newton-Raphson method using as initial value the value from the previous iteration of the SIMPLER algorithm. In the cases where the method tends to fail or to converge slowly, bisection method is using in order to estimate a better initial guess.

3.4 Simulation approach

The computational domain was extended in all directions outside the tunnel in order to minimize the effect of the implied boundary conditions. Its total size was 200 x 60 x 31.2 m. A more extended domain was examined and showed zero impact on the results. The total number of active computational cells was approximately 596,700. The length of the computational cells was varied from 0.184 m inside the ignition zone to 0.194 m at the limits of the premixed area (5 meters from the ignition zone) and to 1.262 m at the end of the tunnel. The width and the height of the cells were almost uniform inside the tunnel and approximately equal to 0.08 m. The cells' volume is increased gradually in the area outside the tunnel in order to save computational time. A denser grid of 941,201 cells was also used in order to examine grid independency. In that case the length of the computational cells was equal to 0.1 m inside the premixed area and the width and the height equal to 0.062 m in the entire tunnel.

In all exit planes (lateral, front, back and top) the non-reflecting boundary conditions for the normal velocities is chosen, while for the parallel to the exit planes' velocity components, Neumann boundary conditions are applied. Zero gradient is utilized also for the mass fraction of species. As initial conditions, a stagnant flow field with no turbulence is specified. In the hydrogen-air premixed area an initial mass fraction of hydrogen and oxygen is specified equal to 0.029077 and 0.226148 respectively. Outside this area the mass fraction of oxygen is set equal to 0.232. Nitrogen is the inert specie. The initial temperature and pressure is set equal to those of the experiment, i.e. 295 K and 1.01325 bar respectively in the whole domain. Ignition is modelled by fixing the reaction rate in a cell at the centre of the tunnel, in order the initial amount of fuel to be burned at a determined time. This time was set equal to 0.1 ms.

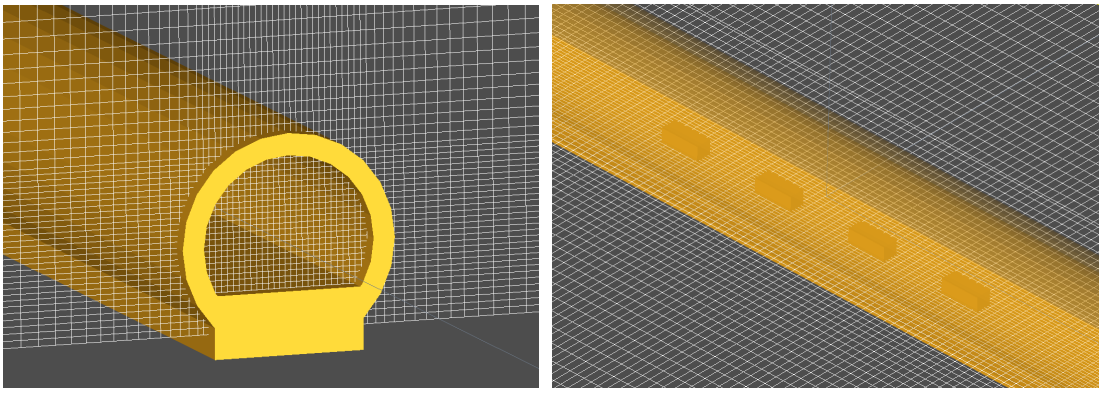

Figure 2. Y-Z and X-Y planes of the computational grid of 596,700 cells.

4.0 RESULTS AND DISCUSSION

Overpressure time history was measured during experiment in four different positions inside the tunnel, at 1.00, 3.61, 10.61 and 30.40 m from the ignition point. In Fig. 3, the comparison of the overpressure history between experiment and simulation is shown for the empty-tunnel case. Two values of parameter ψ were tested: 0.50 and 0.45. Concerning the prediction of the maximum overpressure, a good agreement is exhibit. For the case of ψ=0.50, the ratio of the maximum overpressure between simulation and experimental results is 1.14, 1.20, 1.06 and 1.00 for the closest to the farthest to the ignition sensor respectively. The same ratios for the case of ψ=0.45 are 1.06, 1.11, 0.98 and 0.92. We observe that for ψ=0.45 the predicted maximum overpressures are closer to the experiment at all sensors except the final one at which the case of ψ=0.50 predicts the maximum overpressure perfectly. All relative errors between prediction and experiment for the ψ=0.45 case are lower than 15% which can be considered as satisfactory, given the experimental uncertainty. As a result the value of 0.45 seems to be a better choice for the combustion model parameter ψ. However, the differences between maximum overpressures between these two cases are not significant. Regarding the arrival time of the pressure peak, a good agreement is exhibit in all sensors for both cases.

The results for the case of ψ=0.45 using the denser grid are shown in Fig. 3. We observe that the two curves are almost identical and only slight differences exist. However, denser grids should be examined in order to confirm the grid independency. The same dense grid was also applied to the ψ=0.50 case, and as in the ψ=0.45 case small differences in the results compared to the coarse grid were observed.

Another significant parameter for the evaluation of the deflagration model is the capability to simulate the rate of the pressure rise. This rate can be estimated by the expression [33]:

$$\frac{\partial p}{\partial t} \approx \frac{\left(p_{\max} - p_0\right) - 0.1\left(p_{\max} - p_0\right)}{t_{p\max} - t_{0.1p\max}} \tag{18}$$

The rate of pressure rise and the ratio of the predicted to the experimental rates are presented in Table 1 for each sensor and each value of the parameter ψ. We notice that the agreement between experimental and computational results is much better for the case of ψ=0.50 rather than for the case of ψ=0.45. As shown in Fig. 3 the gradients of overpressure are steep especially at the last sensor where both values of ψ give big divergences from the experiment. In general, cases with steep gradients are more difficult to be simulated accurately. This difficulty can be overcome to some extent by using higher order numerical schemes and dense grids. However, in combustion simulations numerical approach may not be the only reason for this divergence. Combustion process also plays a

significant role in how quick the overpressures will be developed. As a result, an improper combustion model may never achieve to simulate accurately the rate of the pressure rise. The strong dependence between combustion model and pressure rise rate is obvious by observing the ψ parameter effect on the results: The bigger value of ψ leads to a bigger combustion rate (as it can be seen from equation (13)), which leads to a bigger pressure rise rate.

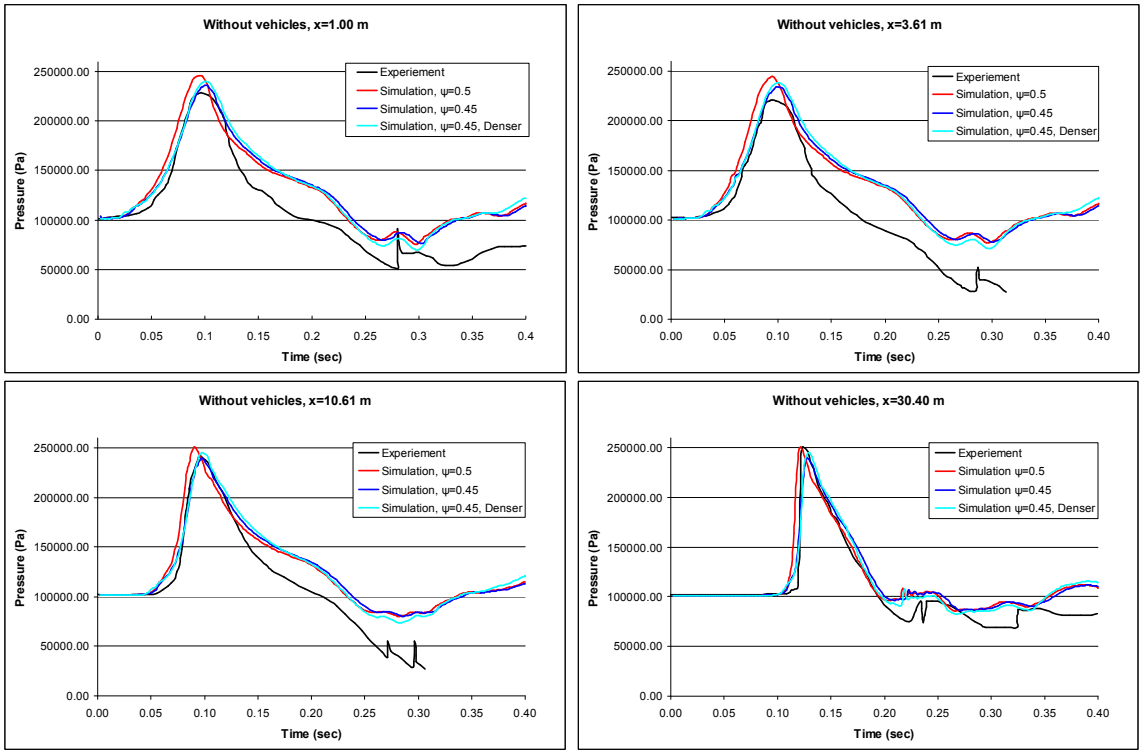

Figure 3. Overpressure time histories for the case without cars at four different positions in the tunnel, for two values (0.50 and 0.45) of the combustion parameter ψ and for a denser grid in the case of ψ=0.45.

Table 1. Rate of pressure rise for the case without vehicles for ψ=0.45 and ψ=0.50.

Sensor location (m)	Rate of pressure rise in experiment (kPa/sec)	Rate of pressure rise in simulation (kPa/sec)		Simulation to Experimental rate of pressure rise	
		ψ=0.50	ψ=0.45	ψ=0.50	ψ=0.45
$x = 1.00$ m	2334	2177	1845	0.93	0.79
$x = 3.61$ m	2525	2477	2007	0.98	0.80
$x = 10.61$ m	4942	4327	2878	0.88	0.58
$x = 30.40$ m	28398	11576	6129	0.41	0.22

In Fig. 3 we also observe discrepancies between the prediction and the experiment after the time that the maximum pressure is reached. In the experiment the pressure drops more rapidly than the simulation at all sensors except for the fourth sensor where this behaviour is less noticeable. This could be due to heat losses, as also mentioned in [33]. Although the timescale of the phenomenon is very small, heat losses can have a considerable impact especially for times after the initial stages of the propagation. A model for heat transfer from the flammable mixture to the walls of the tunnel and from the walls to the outside air was not included in this study.

In Fig. 4, the comparison of the overpressure history between experiment and simulation for the case of the non-empty tunnel and for ψ=0.45 is presented. The three sharp pressure peaks appearing in the experiment at the second sensor at times 0.05 s, 0.085s and 0.094 s have been neglected in the analysis as their shape indicates that they can not be considered as reliable measurements. The diagrams reveal that the predicted maximum overpressure for the positions x=1.0 m and x=3.61 m is quite satisfactory. At the other two positions a small underprediction of the simulation is observed. The ratio of the simulation maximum overpressure to the experimental one is 0.98, 0.96, 0.90 and 0.91 for the closest to the farthest to the ignition sensor respectively. The arrival time values of the pressure peak in the experiment and in the simulation are very close. However, a small delay in the simulation results is observed.

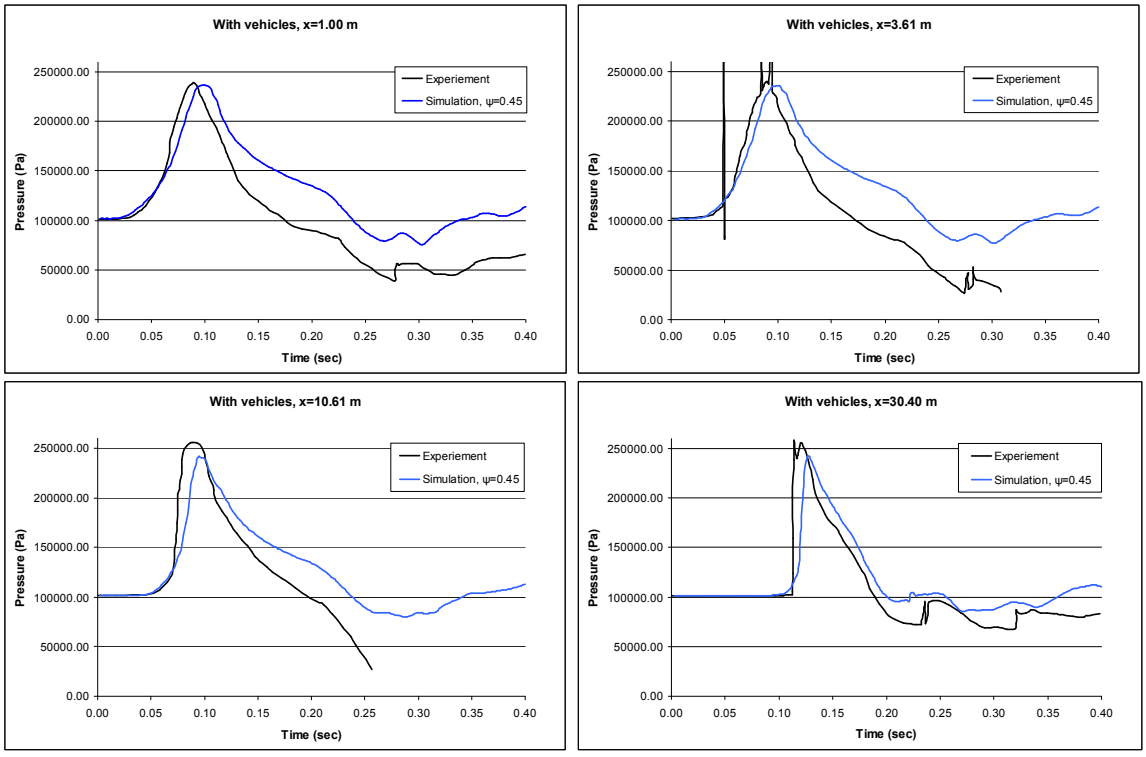

Figure 4. Overpressure time history for the case without cars at four different positions and ψ=0.45.

In Table 2 the rate of pressure rise is presented along with the ratio of the predicted rate to the experimental one for each sensor. As expected from the results of the empty tunnel case, the agreement is not very good.

Table 2. Rate of pressure rise for the case with vehicles.

Sensor location (m)	Rate of pressure rise in experiment (kPa/sec)	Rate of pressure rise in simulation (kPa/sec)	Simulation to Experimental rate of pressure rise
$x = 1.00$ m	2754	2123	0.77
$x = 3.61$ m	2979	2233	0.75
$x = 10.61$ m	6244	3936	0.63
$x = 30.40$ m	16848	10137	0.60

5.0 CONCLUSIONS

During the last several years hydrogen has been a subject of massive research as a potential energy

carrier. If hydrogen is to be used in practical applications, a thorough risk assessment is required since it is a flammable gas capable of causing deflagrations or even detonations. For this purpose CFD may be an accurate and reliable numerical tool. Any CFD code should be validated in order to evaluate its capabilities and limitations. In this work, the ADREA-HF CFD code is evaluated against a hydrogen deflagration in a 78.5 m model of a tunnel. The incorporated combustion model is based on the turbulent flame speed concept. Special attention is given to the modelling of the turbulence generated by the flame front itself, to the preferential diffusion instability and to the fractal structure of the flame front. In order to take these effects into account, a modified Yakhot's equation was used. Two cases were examined: one of a complete empty tunnel and one with four vehicles located near the ignition point. For the empty tunnel case a sensitivity analysis for the combustion parameter ψ and for the mesh resolution was performed.

The code was found capable of simulating the combustion process and predicting the generated overpressures. For the empty tunnel case the sensitivity analysis of the parameter ψ showed that even a small change in its value ranged from 0.45 to 0.50 can have impact on the simulating results. The case with ψ=0.45 predicted the maximum overpressures better than the case with ψ=0.50. On the other hand, the case with ψ=0.50 led to a better prediction of the rate of the pressure rise. This behavior can been explained by the fact that bigger values of ψ leads to bigger values of reaction rate.

The sensitivity analysis for the mesh resolution showed that the results with the dense grid had no significant differences compared to the coarse grid.

In both cases, after the maximum pressure has been achieved, the pressure drops more rapidly in the experiment than in the simulation. A possible cause for this disagreement is the fact that the heat transfer losses through the tunnel were not modelled in the simulations. The rate of the pressure rise is underestimated compared to the experiment. Concerning the value of the maximum pressure and the time it appears, the agreement between experimental and computational results is satisfactory in both empty and non empty cases.

In the future, further evaluation of the combustion model should be made. Cases with different mixture composition (e.g. lean mixtures) and geometrical characteristics need to be tested. The effect of the turbulence model and the numerical schemes should also be examined.

ACKNOWLEDGMENTS

The authors would like to acknowledge the project HyIndoor ("Pre-normative research on safe indoor use of fuel cells and hydrogen systems", Grant agreement no: 278534) for the support of this work.

REFERENCES

1. Venetsanos, A.G., Huld, T., Adams, P. and Bartzis, J.G., Source, dispersion and combustion modelling of an accidental release of hydrogen in an urban environment, *Journal of hazardous materials*, **105**, No. 1, 2003, pp. 1-25.
2. Bjerketvedt, D. and Mjaavatten, A., A hydrogen air explosion in a process plant: a case history, 5th International Conference on hydrogen safety, 2005.
3. Bartzis, J. G., ADREA-HF: A three-dimensional finite volume code for vapour cloud dispersion in complex terrain, Report EUR 13580 EN, 1991.
4. Venetsanos, A.G., Papanikolaou, E. and Bartzis, J.G., The ADREA-HF CFD code for consequence assessment of hydrogen applications, *International Journal of Hydrogen Energy*, **35**, No. 8, 2010, pp. 3908-3918.
5. Ciccarelli, G. and Dorofeev, S., Flame acceleration and transition to detonation in ducts, *Progress in Energy and Combustion Science*, **34**, No. 4, 2008, pp. 499-550.

6. Groethe, M., Merilo, E., Colton, J., Chiba, S., Sato, Y. and Iwabuchi, H., Large-scale hydrogen deflagrations and detonations, *International Journal of Hydrogen Energy*, **32**, No. 13, 2007, pp. 2125-2133.
7. Sato, Y., Iwabuchi, H., Groethe, M., Merilo, E. and Chiba, S., Experiments on hydrogen deflagration, *Journal of power sources*, **159**, No. 1, 2006, pp. 144-148.
8. Yakhot, V. and Orszag, S., Renormalization group analysis of turbulence. I. Basic theory, *Journal of scientific computing*, **1**, No. 1, 1986, pp. 3-51.
9. Molkov, V., Makarov, D. and Schneider, H., LES modelling of an unconfined large-scale hydrogen–air deflagration, *Journal of Physics D: Applied Physics*, **39**, No. 20, 2006, pp. 4366.
10. Molkov, V.V., Makarov, D.V. and Schneider, H., Hydrogen-air deflagrations in open atmosphere: large eddy simulation analysis of experimental data, *International journal of hydrogen energy*, **32**, No. 13, 2007, pp. 2198-2205.
11. Molkov, V., Verbecke, F. and Makarov, D., LES of Hydrogen-Air Deflagrations in a 78.5-m Tunnel, *Combustion Science and Technology*, **180**, No. 5, 2008, pp. 796-808.
12. Zimont, V., Polifke, W., Bettelini, M. and Weisenstein, W., An efficient computational model for premixed turbulent combustion at high Reynolds numbers based on a turbulent flame speed closure, *Journal of engineering for gas turbines and power*, **120**, No. 3, 1998, pp. 526-532.
13. Lipatnikov, A.N. and Chomiak, J., Turbulent flame speed and thickness: phenomenology, evaluation, and application in multi-dimensional simulations, *Progress in energy and combustion science*, **28**, No. 1, 2002, pp. 1-74.
14. Schmid, H.P., Habisreuther, P. and Leuckel, W., A model for calculating heat release in premixed turbulent flames, *Combustion and Flame* , **113**, No. 1-2, 1998, pp. 79-91.
15. Herweg, R. and Maly, R.R., A Fundamental Model for Flame Kernel Formation in S.I. Engines, 1992, Society of Automotive Engineers, SAE 922243.
16. Kawanable, H., Masabiro, S., Takasbi, T. and Yusoff, A., CFD simulation for predicting combustion and pollutant formation in a homogeneous charge spark-ignition engine, Int. Symposium COMODIA, vol. 98, 1998, pp. 233-238.
17. Yakhot, V., Propagation velocity of premixed turbulent flames, *Combustion Science and Technology*, **60**, No.1-3, 1988, pp. 191-214.
18. Karlovitz, B., Denniston Jr, D.W. and Wells, F.E., Investigation of turbulent flames, *The Journal of Chemical Physics*, **19**, 1951, pp. 541-547.
19. Gostintsev, Y.A., Istratov, A.G and Shulenin, Y.V., Self-similar propagation of a free turbulent flame in mixed gas mixtures, *Combustion, Explosion, and Shock Waves*, **24**, No.5, 1988, pp. 563-569.
20. Huahua, X., Makarov, D., Sun, J. and Molkov, V., Experimental and numerical investigation of premixed flame propagation with distorted tulip shape in a closed duct, *Combustion and Flame*, **159**, No. 4, 2012, pp. 1523-1538.
21. Zimont, V.L. and Lipatnikov, A.N., A Numerical Model of Premixed Turbulent Combustion of Gases, *Chemical Physics Reports*, **14**, No. 7, 1995, pp. 993-1025.
22. Molkov, V., Fundamentals of hydrogen safety engineering, 2012, BookBoon, ISBN 978-87-403-0226-4.
23. Dahoe, A.E., Laminar burning velocities of hydrogen–air mixtures from closed vessel gas explosions, *Journal of loss prevention in the process industries*, **18**, No.3, 2005, pp. 152-166.
24. Makarov, D., Verbecke, F., Molkov, V., Kotchourko, A., Lelyakin, A., Yanez, J., Baraldi, D., Heitsch, M., Efimenko, A. and Gavrikov, A., An intercomparison of CFD models to predict lean and non-uniform hydrogen mixture explosions, *International Journal of Hydrogen Energy*, **35**, No. 11, 2010, pp. 5754-5762.
25. Moult, A., Spalding, D.B. and Markatos, N.C.G, Solution of flow problems in highly irregular domains by the finite-difference method, *Transactions of the Institution of Chemical Engineers*, **57**, No. 3, 1979, pp. 200-204.

26. Bartzis, J.G., Venetsanos, A.G., Varvayanni, M., Catsaros, N. and Megariton, A., ADREA-I: A three-dimensional transient transport code for complex terrain and other applications, *Nuclear Technology*, **94**, No. 2, 1991, pp. 135-148.
27. Patankar, S.V., Numerical transfer and fluid flow, Hemisphere Publishing Corporation, 1980, Taylor and Francis group, New York.
28. Kovalets, I.V., Andronopoulos, S., Venetsanos, A.G. and Bartzis, J.G., Optimization of the numerical algorithms of the ADREA-I mesoscale prognostic meteorological model for real-time applications, *Environmental Modelling & Software*, **23**, No.1, 2008, pp. 96-108.
29. Waterson, N.P. and Deconinck, H., Design principles for bounded higher-order convection schemes–a unified approach, *Journal of Computational Physics*, **224**, No. 1, 2007, pp. 182-207.
30. Chatelain, A., Ducros, F. and Metais, O., LES of turbulent heat transfer: proper convection numerical schemes for temperature transport, *International journal for numerical methods in fluids*, **44**, No. 9, 2004, pp. 1017-1044.
31. Khosla, P.K. and Rubin, S.G., A diagonally dominant second-order accurate implicit scheme, *Computers & Fluids*, **2**, No. 2, 1974, pp. 207-209.
32. Versteeg, H.K., and Malalasekera, W., An introduction to computational fluid dynamics: the finite volume method, 2007, Prentice Hall.
33. Baraldi, D., Kotchourko, A., Lelyakin, A., Yanez, J., Middha, P., Hansen, O.R., Gavrikov, A., Efimenko, A., Verbecke, F., Makarov, D. and Molkov, V., An inter-comparison exercise on CFD model capabilities to simulate hydrogen deflagrations in a tunnel, *International Journal of Hydrogen Energy*, **34**, No. 18, 2009, pp. 7862-7872.